nature climate change

Article

https://doi.org/10.1038/s41558-024-02035-w

Biodiversity buffers the response of spring leaf unfolding to climate warming

Received: 10 October 2023

Accepted: 13 May 2024

Published online: 21 June 2024



Check for updates

Pengju Shen @ 1,2,14, Xiaoyue Wang @ 1,2,14, Constantin M. Zohner @ 3, Josep Peñuelas • 4,5, Yuyu Zhou • 6, Zhiyao Tang • 7, Jianyang Xia • 8, Hua Zheng **®**⁹, Yongshuo Fu **®**¹⁰, Jingjing Liang¹¹, Weiwei Sun **®**¹²⊠, Yongguang Zhang ^{® 13} ≥ & Chaoyang Wu ^{® 1,2} ≥

Understanding the sensitivity of spring leaf-out dates to temperature (S_T) is integral to predicting phenological responses to climate warming and the consequences for global biogeochemical cycles. While variation in S_T has been shown to be influenced by local climate adaptations, the impact of biodiversity remains unknown. Here we combine 393,139 forest inventory plots with satellite-derived S_T across the northern hemisphere during 2001– 2022 to show that biodiversity greatly affects spatial variation in S_T and even surpasses the importance of climate variables. High tree diversity significantly weakened S_T , possibly driven by changes in root depth and soil processes. We show that current Earth system models fail to reproduce the observed negative correlation between S_T and biodiversity, with important implications for phenological responses under future pathways. Our results highlight the need to incorporate the buffering effects of biodiversity to better understand the impact of climate warming on spring leaf unfolding and carbon uptake.

Plant phenology is one of the most sensitive indicators of climate change and greatly affects interannual variations in carbon uptake of terrestrial ecosystems^{1,2}. Over recent decades, climate warming has led to strong advances in spring leaf-out dates^{3,4}. The responsiveness of spring phenology to climate change is typically quantified via measuring the temperature sensitivity of leaf-out (S_T , leaf-out advance in days per degree of air temperature warming). S_T is the optimal strategy evolved by plants under the selection pressure of historical climate information in the local environment, and its variations reflect adaptive adjustments to climate change for optimizing their life cycles^{5,6}. Due to its role in determining the extent of phenological changes in response to future climate warming, S_T has attracted extensive attention in observational records and warming experiments^{5,7-9}. Understanding temporal and spatial variation in S_T is critical to better comprehend phenological feedbacks to climate change, such as effects on carbon sequestration⁷, surface albedo and the energy budget^{7,10}. Furthermore, it is of paramount importance for evaluating and simulating the dynamics of ecosystems in climate change research⁸, as well as for enhancing

1Key Laboratory of Land Surface Pattern and Simulation, Institute of Geographic Sciences and Natural Resources Research, Chinese Academy of Sciences, Beijing, China. ²University of the Chinese Academy of Sciences, Beijing, China. ³Department of Environmental Systems Science, Institute of Integrative Biology, ETH Zurich, Zurich, Switzerland. 4CSIC, Global Ecology Unit CREAF-CSIC-UAB, Bellaterra, Barcelona, Spain. 5CREAF, Barcelona, Spain. ⁶Department of Geological and Atmospheric Sciences, Iowa State University, Ames, IA, USA. ⁷Institute of Ecology, College of Urban and Environmental Science and Key Laboratory for Earth Surface Processes of Ministry of Education, Peking University, Beijing, China. 8Zhejiang Tiantong Forest Ecosystem National Observation and Research Station, Institute of Eco-Chongming, School of Ecological and Environmental Sciences, East China Normal University, Shanghai, China. 9State Key Laboratory of Urban and Regional Ecology, Research Center for Eco-Environmental Sciences, Chinese Academy of Sciences, Beijing, China. 10 College of Water Sciences, Beijing Normal University, Beijing, China. 11 Forest Advanced Computing and Artificial Intelligence Laboratory, Department of Forestry and Natural Resources, Purdue University, West Lafayette, IN, USA. 12 Department of Geography and Spatial Information Techniques, Ningbo University, Ningbo, China. 13 International Institute for Earth System Sciences, Jiangsu Center for Collaborative Innovation in Geographical Information Resource Development and Application, Nanjing University, Nanjing, China. 14These authors contributed equally: Pengju Shen, Xiaoyue Wang. ⊠e-mail: sunweiwei@nbu.edu.cn; yongguang_zhang@nju.edu.cn; wucy@igsnrr.ac.cn

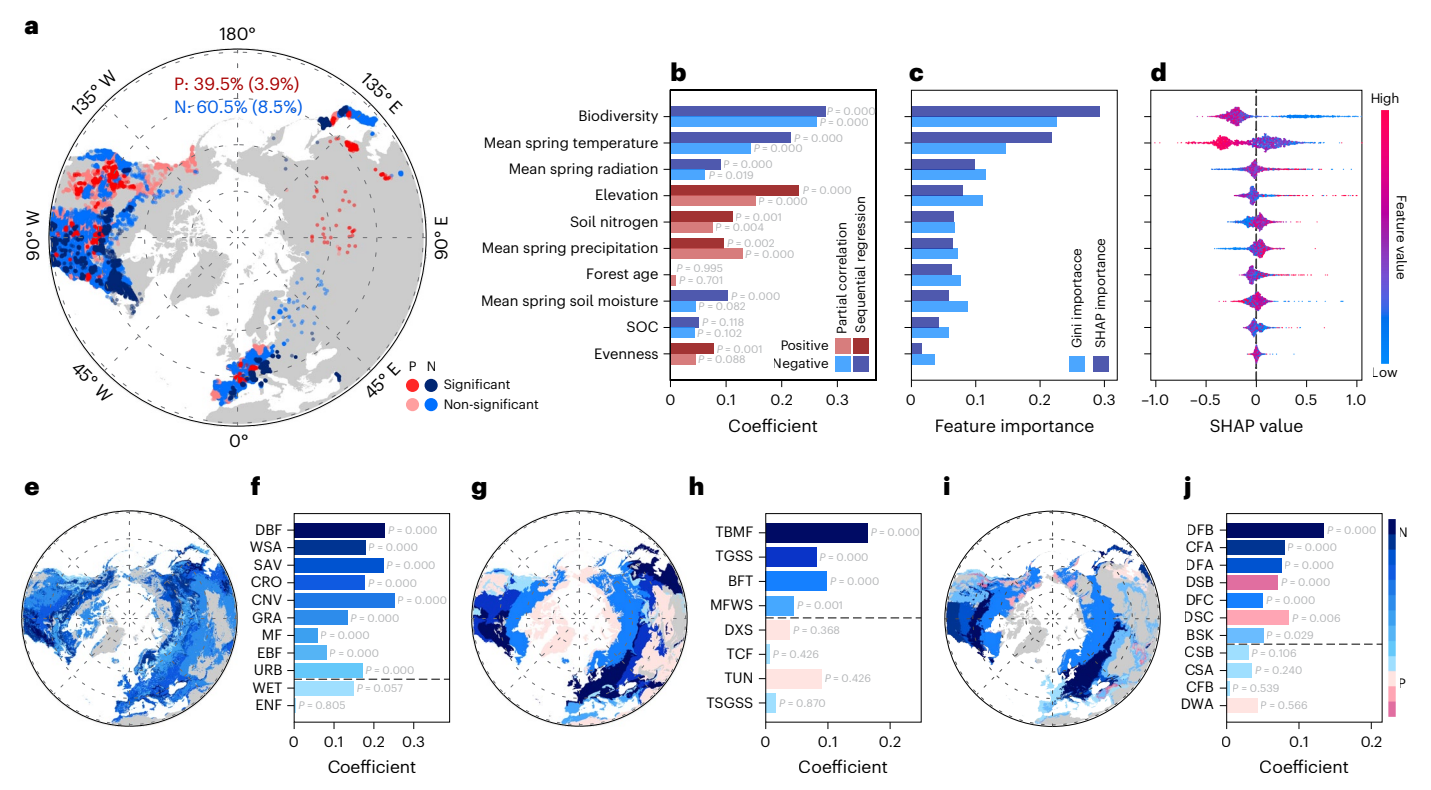


Fig. 1| **Negative correlations between biodiversity and** S_{T} **.** \mathbf{a} , \mathbf{e} - \mathbf{j} , The results of the partial correlation analysis for each plot (\mathbf{a}), plant functional type (\mathbf{e} , \mathbf{f}), biome (\mathbf{g} , \mathbf{h}) and climate (\mathbf{i} , \mathbf{j}) (the full names of the abbreviations in \mathbf{f} , \mathbf{h} , \mathbf{j} can be found in Supplementary Tables 4–6). \mathbf{b} , The coefficients of the global partial correlation and sequential regression. \mathbf{c} , The importance of each feature based on Gini coefficients and the mean absolute value of SHAP. \mathbf{d} , SHAP values based

on the global random forest model. P, positive effect; N, negative effect. In $\bf a$, the overall percentages of positive and negative correlations and the percentages of significant correlations (in parentheses) are given. The grey dashed lines in $\bf f,h,j$ mark the transition from significant to non-significant results at P < 0.05. The significance was based on $\bf t$ statistics using a two-tailed test. To control the false discovery rate, the Benjamini–Hochberg method was employed in $\bf a,f,h,j$.

global dynamic vegetation models, global climate models and land surface models 6,11 . Declines in S_T have been observed in several tree species over recent decades. Yet, although decreased winter chilling has been suggested as a possible factor, the underlying causes remain poorly understood 9 . While previous studies have mostly focused on the climatic drivers of S_T , we still lack an understanding of the responses of S_T to changes in the biodiversity of animals, plants and microorganisms and the communities they form 12 .

Biodiversity plays a crucial role in regulating the growth and development of vegetation, serving as a key factor in stabilizing and adapting ecosystems to climate change¹³. At a large geographical scale, plant phenology responds to climate and environmental factors, influencing plant growth and resilience while also governing crucial ecosystem functions such as pollination, herbivory and carbon uptake¹⁴. Consequently, warming-induced changes in spring leaf-out may lead to asynchronous interactions among mutualistic partners within communities, affecting food web dynamics and the functioning and stability of ecosystems^{2,3,15,16}. In particular, high biodiversity can influence the phenological plasticity of individual plants, enhance the adaptability of plants to climatic shifts, diminish the likelihood of phenological discordance, and affect the species assemblage and functional heterogeneity of plant communities, thereby mitigating the effects of climate change on ecosystem performance^{17,18}. For example, different genotypes or genera of plants can adapt to variations in temperature and moisture by altering gene expression, hormone levels, leaf area and other parameters that affect phenology¹⁹. Different species have different responses to cope with environmental fluctuations, and higher temporal complementarity and asynchrony among species can augment their resistance to drought²⁰. Regions with high biodiversity

thus typically have stabler ecosystem responses to climate change, whereas the loss of diversity may aggravate plant phenological shifts caused by climate change ^{13,16,17}. In this study, we therefore aimed to test whether biodiversity buffers the sensitivity of trees to climate warming and how interactions between biodiversity and climate change affect northern-hemisphere-wide phenological variation.

We compiled species richness data from the Global Forest Biodiversity Initiative (GFBI) in the middle and high latitudes of the northern hemisphere, incorporating 393,139 unique forest inventory plots that span various forest types and species, to characterize biodiversity (Supplementary Fig. 1). Satellite-derived leaf-out data from 2001–2022 came from the Moderate-Resolution Imaging Spectroradiometer (MODIS). We also gathered spatially explicit climate and soil data from 2000-2022, as well as gross primary production (GPP) data from 15 Trendy models for 2001–2021 and 13 Coupled Model Intercomparison Project Phase 6 (CMIP6) models for 2015–2100 (Supplementary Tables 1–3). For each forest plot, we calculated the optimal spring pre-season period using partial correlation analysis and calculated S_T using ordinary least squares regression (Supplementary Fig. 2). We then used partial correlation, a sequential regression model, spatial autoregressive models, a structural equation model (SEM) and machine learning to determine the influence of biodiversity on S_T and its underlying mechanisms at regional and global levels (Methods).

Results

The partial correlation analysis showed a predominantly negative correlation between biodiversity and S_T at the local scale after removing the effects of spring temperature, radiation, precipitation, soil moisture, soil organic carbon (SOC), soil nitrogen, forest age and elevation

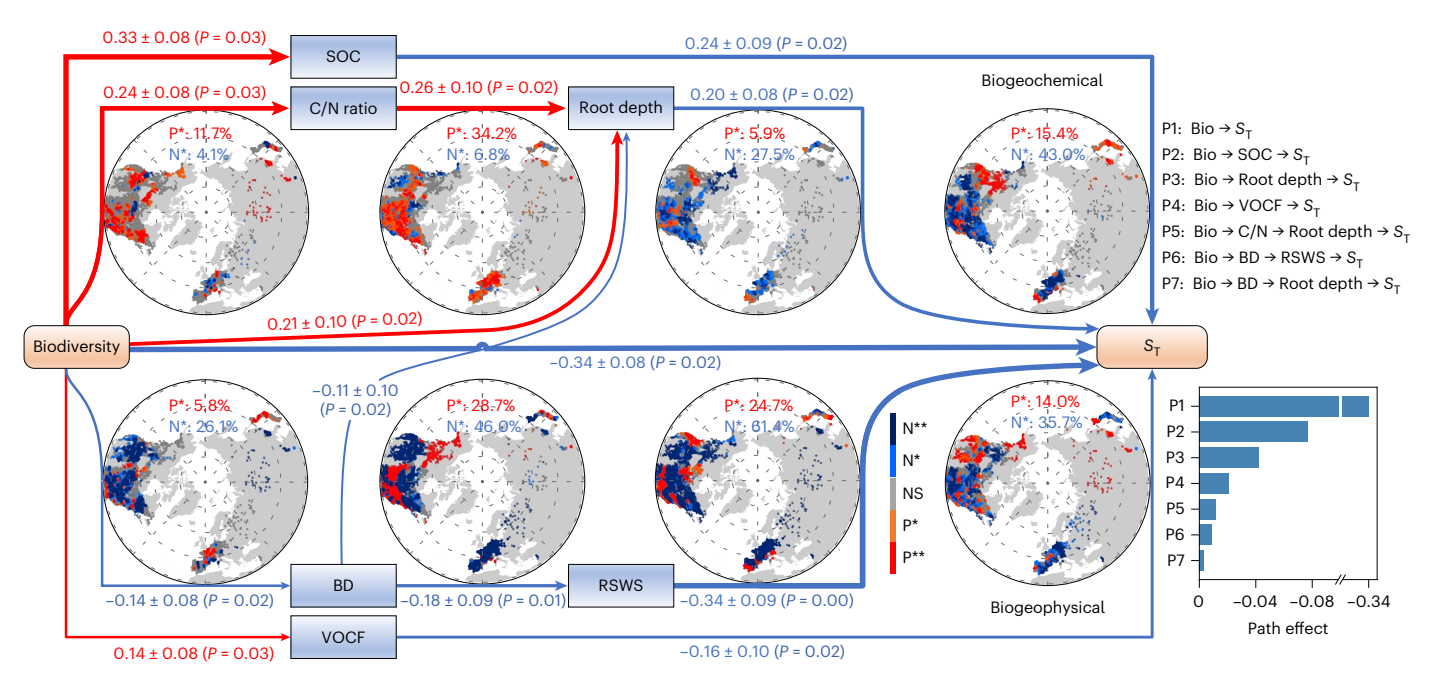


Fig. 2 | **Mechanisms underlying the negative correlation between biodiversity and S_T.** The results of the partial correlation analysis and SEM are shown. The coefficients on the paths of the SEM are standardized, and the circular maps on the paths represent the spatial distributions of the partial correlation results. The thickness of path arrows corresponds to the size of path coefficient, and the color to the sign, red for positive and blue for negative.

The bar chart represents the direct and indirect effects. NS, not significant; BD, soil bulk density. The significance was based on t statistics using a two-tailed test. To control the false discovery rate, the Benjamini–Hochberg method was employed in all analyses. **P < 0.01; *P < 0.05. $\chi^2 = 48.86 \pm 17.05$; goodness-of-fit index, 0.93 \pm 0.02; root mean square error of approximation, 0.06 \pm 0.04; Akaike information criterion. 89.02 \pm 0.34.

(Fig. 1a), with 60.5% of the correlations being negative. Moreover, 8.5% of the local correlations were significantly negative (P < 0.05), while significant positive correlations were found for only 3.9% of the correlations. The partial correlation analysis showed consistent results at the levels of plant functional types (Fig. 1e,f), forest biomes (Fig. 1g,h) and Köppen-Geiger climate zones (Fig. 1i,j). For example, negative correlations were found for all 11 plant functional types, with 9 being significant. Similarly, four of the eight biomes showed a negative correlation, and all four correlations were significant, with only deserts and xeric shrublands (DXS) and tundra (TUN) showing a non-significant positive correlation. Biodiversity and S_{T} were also negatively correlated in 8 of 11 climate zones (five correlations were significant) and exhibited significant positive correlations in 2 zones (DSB (continental.) dry summer, warm summer) and DSC (continental, dry summer, cold summer)). Furthermore, a negative correlation between biodiversity and S_T was observed across different plant functional types, as well as across various biomes and climate zones (Supplementary Fig. 3). In the global analysis covering all plots, we controlled for evenness variables, in addition to the previously mentioned environmental factors. Consistent results were obtained from partial correlation analysis, a sequential regression model, and spatial lag and spatial error models, indicating an overall negative biodiversity-S_T effect (Fig. 1b and Supplementary Fig. 4).

We then analysed the relative importance of biodiversity in determining the changes in S_T using machine learning (random forest and Extreme Gradient Boosting (XGBoost) models). We found that biodiversity was a more important driver of S_T than were spring temperature, precipitation, solar radiation, soil moisture, SOC, soil nitrogen, forest age, elevation and evenness (Fig. 1c,d and Supplementary Fig. 5). Additionally, the Shapley Additive Explanations (SHAP) values of the random forest and XGBoost models revealed that plots with higher biodiversity levels often exhibited a negative relationship between biodiversity and S_T , while regions with lower biodiversity levels might have a positive biodiversity- S_T relationship. Overall, a predominance

of negative correlations was observed, aligning with the results from the partial correlation and sequential regression analyses. Both feature importance metrics (Gini importance and SHAP importance), along with the absolute coefficients of the partial correlation and sequential regression, consistently indicate that biodiversity is the most important driver of S_T .

We also used grid-form species richness data to ensure spatial consistency with the scale of climate and other datasets, providing a better match with point-form species evenness data. We replicated the same analysis, controlling for the influences of spring temperature, precipitation, solar radiation, soil moisture, SOC, soil nitrogen, forest age, elevation and evenness in all analyses. The results remained consistent with those obtained from plot datasets, revealing a negative effect of biodiversity on $S_{\rm T}$ (Supplementary Fig. 6).

To test the possible mechanisms through which biodiversity may affect S_T , we applied an SEM and partial correlation analysis (Fig. 2). We calculated the direct effects of biodiversity on S_T in the SEM and the indirect effects through different pathways. The results indicate a strong direct effect of biodiversity. In addition, root depth, SOC concentration, the soil carbon-to-nitrogen (C/N) ratio and soil physical properties (including bulk density and volumetric fraction of coarse fragments (VOCF)) may be potential intermediaries between biodiversity and phenological responsiveness. For example, biodiversity and the C/N ratio were mostly positively correlated, with 11.7% and 4.1% of correlations being significantly positive and negative, respectively. The correlation between the C/N ratio and root depth was also positive, with 34.2% of the correlations significantly positive and only 6.8%of the correlations significantly negative. In comparison, root depth and S_T were generally negatively correlated. Similarly, a higher SOC concentration was associated with increased biodiversity, but SOC concentration and S_T were negatively correlated. Soil physical properties may also contribute to the negative relationship between biodiversity and S_T . Biodiversity and bulk density, bulk density and the rate of soil warming in spring (RSWS), and RSWS and S_T were each consistently

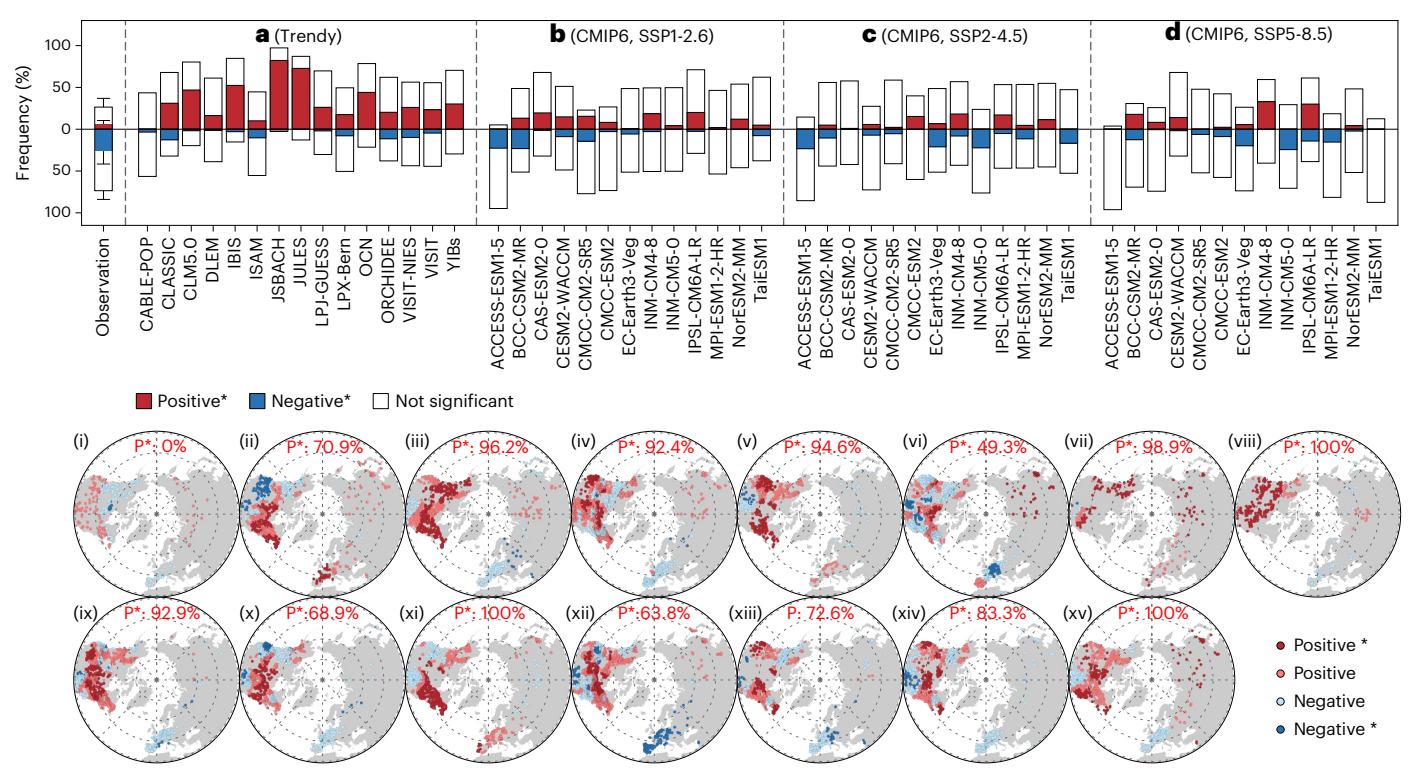


Fig. 3 | Evaluation of model performances on S_T with biodiversity. a-d, The results for 15 Trendy models (a) and 13 CMIP6 models under different SSPs (SSP1-2.6 (b), SSP2-4.5 (c) and SSP5-8.5 (d)) (see Supplementary Tables 2 and 3 for the model details). The 'Observation' bar in a is derived from the analysis results of 11 sets of resampled data (Supplementary Fig. 11), presented as mean values

 \pm standard deviation. The subpanels (i)–(xv) in **a** represent spatial distribution results for the 15 Trendy models. The numbers in these figures are percentages of significant positive correlations with respect to all significant correlations. The significance level was established at P< 0.05, determined by t statistics in a two-tailed test.

negatively correlated, with the percentages of significant positive/negative correlations being 5.8%/26.1%, 28.7%/46.0% and 24.7%/61.4%, respectively. In contrast to bulk density, a higher VOCF was associated with increased biodiversity, and biodiversity increased as $S_{\rm T}$ decreased, because VOCF and $S_{\rm T}$ were negatively correlated. Overall, both the direct and the indirect pathways support the negative correlation between biodiversity and $S_{\rm T}$.

We further tested whether Earth system models (15 Trendy models with results over 2001–2021 and 13 CMIP6 models over 2016–2100) can reproduce the negative correlation between S_T and biodiversity (Fig. 3). We found that most Trendy models do not capture the observed relationships, with 13 of 15 models simulating predominantly positive correlations (positive correlations exceeding 60%) and only one of the models reproducing the extent of observed negative correlations (negative correlations exceeding 60%, the CABLE-POP model). The spatial variation in the correlations simulated by the Trendy models is shown in Fig. 3a(i)-(xv). The CMIP6 models also failed to represent the negative correlation between S_T and biodiversity (Fig. 3b-d). We found that only 4 of 13 models (ACCESS-ESM1-5, BCC-CSM2-MR, EC-Earth3-Veg and TaiESM1) had negative S_T -biodiversity relationships exceeding 60% under Shared Socio-economic Pathway (SSP) 1-2.6. The number of correct models increased to 5-7 for SSP2-4.5 and SSP5-8.5. Spatial distributions of the CMIP6 models are provided in Supplementary Figs. 7–9. We also tested for spatial consistency between the observations and simulations and found that most models did not closely match the observed biodiversity effects (Extended Data Fig. 1).

Discussion

Our findings demonstrate a widespread buffering effect of biodiversity on the sensitivity of spring leaf-out dates to climate warming, with weaker responses of spring leaf-out to warming in forests with multiple

species. Our models further show that biodiversity is more important than climate in driving spatial variation in S_T (Fig. 1b–d and Supplementary Fig. 5), highlighting the importance of considering biodiversity when predicting the effects of climate change on spring phenology and ecosystem productivity. We further showed that current Earth system models cannot reproduce the observed buffering effect of biodiversity on spring phenological sensitivity. Accounting for spatial and temporal variation in species richness will thus be of great importance to better understanding the extent of shifts in foliar phenology under climate change as well as the consequences for ecosystem functioning.

We found that biodiversity has a strong direct impact on S_T in our study. We observed that in forests with higher biodiversity, the sensitivity of tree leaf unfolding to climate warming is lower. This suggests that in ecosystems with higher biodiversity, the timing of spring leaf unfolding remains more stable in the face of warming, consistent with recent research^{16,17,21}. This direct effect can be partly attributed to the presence of a greater variety of species and individuals in biodiverse forests, where different tree species may have distinct growth seasons and leaf unfolding times. This seasonal asynchrony may, to some extent, slow down the overall response of the ecosystem to rising temperatures 14,22 . Consequently, the entire ecosystem exhibits lower average S_T . Conversely, in biomes or climate zones with lower biodiversity, often dominated by a few key species, the response is more uniform, and leaf unfolding is more directly and significantly influenced by temperature increase (Supplementary Fig. 3). In such cases, biodiversity may not be able to exert a buffering effect, as observed in biomes such as deserts and xeric shrublands (DXS) and tundra (TUN), as well as cold and dry climate zones (DSC and DSB) (Fig. 1g-j).

While our analyses suggest a strong direct impact of biodiversity on S_T , they also suggest that biogeophysical and biogeochemical factors may contribute to the decrease in S_T with increasing biodiversity. We

found that high biodiversity correlates with deeper roots, which may facilitate access to soil nutrients and moisture during spring²³. The enhanced water supply may in turn reduce trees' sensitivity to temperature early in the growing season, buffering against warming-induced shifts in foliar phenology¹³ (Extended Data Fig. 2). In agreement with this, experiments and observations have shown reduced leaf-out sensitivity to warming under drought conditions^{1,9}. Our results also agree with studies reporting an increased importance of soil moisture in determining the distribution of vegetation and SOC in cold regions where warming is more pronounced²⁴.

Our findings also support the idea that higher biodiversity enhances the SOC concentrations in diverse forests by fixing more carbon^{13,18,25}. This may be due to improved soil physicochemical properties, such as VOCF and pH (Extended Data Fig. 3), which in turn accelerate the activities of both plants and soil microorganisms^{12,25,26}. Enhanced soil fertility is advantageous for plants because it promotes plant growth and enables roots to anchor more deeply, facilitating more effective adaptation to temperature changes¹³. Increasing soil fertility can in turn increase the diversity of plants and soil microorganisms, increasing the stability and resilience of ecosystems. We also found that higher biodiversity increases the C/N ratio, which may limit the availability of nitrogen for plants and cause them to allocate more carbon to root growth to enhance the uptake of water and nutrients while reducing foliar growth to save energy for photosynthesis and transpiration²⁷.

Higher biodiversity may contribute to improvements in soil biogeophysical properties, including enhanced soil aeration, thermal conductivity and water retention, which may be associated with increased soil microbial activity and plant root growth^{23,26}. The improvement of soil physical properties, especially water retention and buffering capacity, has been demonstrated to enhance the resistance of plants to stress, thus alleviating the response of plants to warming and consequently improving phenological stability^{23,25}. Our results also showed that S_T becomes less dependent on warming under wetter conditions induced by higher biodiversity (Extended Data Fig. 2). Better soil aeration and thermal conductivity may increase RSWS and its variability, causing a higher frost risk. To avoid such risks, plants may therefore increasingly rely on other signals, such as photoperiod and higher chilling requirements, leading to declines in $S_T^{5,28}$. The enhancement of soil physical properties affects the growth of plant roots and the retention of SOC and soil nitrogen^{23,25}, and increased rooting depth and supply with soil nutrients are likely to drive phenological stability and reduce S_{τ} (Fig. 2).

Predictive models of vegetation leaf phenology are a crucial component of land surface models and dynamic global vegetation models, as well as global climate models that use soil–vegetation–atmosphere transfer schemes of Negetation phenology on the interannual variations and trends in land carbon–water cycles and land–atmosphere exchanges, but they still pose challenges in terms of phenology model accuracy Decause S_T determines the extent of phenological responses to future climate warming, it is crucial for phenological simulations to consider this effect Decause S_T of the buffering effects of biodiversity on S_T are not considered, inaccuracies in phenological simulations may occur, thereby affecting the characterization of ecosystem functions. This may be why many CMIP6 and Trendy models have failed to reproduce the negative biodiversity– S_T correlations (Fig. 3).

Our findings show that the sensitivity of spring leaf-out to warming is lower in more diverse forests, suggesting an important buffering effect of biodiversity on the phenological sensitivity of trees to climate change. The biodiversity effects on phenological sensitivity may be both direct and indirect. In diverse forests, the high diversity in temperature sensitivity among species and individuals may lead to a lower average temperature sensitivity than in less diverse forests, where single species dominate the observed community sensitivity. In addition, the biodiversity effects could be mediated by soil physicochemical properties, which may stabilize phenology by enhancing nutrient

supply, stress tolerance and productivity ^{17,18,20}. Higher productivity in diverse forests may also lead to changes in ecosystem function due to shifts in species composition and community succession, water balance and climatic feedbacks³⁰. The inability of Earth system models to reproduce the observed buffering effect of tree diversity on phenological sensitivity highlights the need to represent biodiversity if we are to accurately predict ecosystem responses to climate change. Our findings thus underscore the fundamental importance of biodiversity in our understanding of phenological changes and the maintenance of ecosystem functioning under climate change.

Online content

Any methods, additional references, Nature Portfolio reporting summaries, source data, extended data, supplementary information, acknowledgements, peer review information; details of author contributions and competing interests; and statements of data and code availability are available at https://doi.org/10.1038/s41558-024-02035-w.

References

- Gu, H. et al. Warming-induced increase in carbon uptake is linked to earlier spring phenology in temperate and boreal forests. *Nat. Commun.* 13, 3698 (2022).
- Peñuelas, J., Rutishauser, T. & Filella, I. Phenology feedbacks on climate change. Science 324, 887–888 (2009).
- 3. Peñuelas, J. & Filella, I. Responses to a warming world. *Science* **294**, 793–795 (2001).
- Menzel, A. et al. European phenological response to climate change matches the warming pattern. Glob. Change Biol. 12, 1969–1976 (2006).
- Wang, T. et al. The influence of local spring temperature variance on temperature sensitivity of spring phenology. Glob. Change Biol. 20, 1473–1480 (2014).
- Bennie, J., Kubin, E., Wiltshire, A., Huntley, B. & Baxter, R. Predicting spatial and temporal patterns of bud-burst and spring frost risk in north-west Europe: the implications of local adaptation to climate. Glob. Change Biol. 16, 1503–1514 (2010).
- Gao, M. et al. Three-dimensional change in temperature sensitivity of northern vegetation phenology. *Glob. Change Biol.* 26, 5189–5201 (2020).
- Shen, M. et al. Earlier-season vegetation has greater temperature sensitivity of spring phenology in northern hemisphere. PLoS ONE 9. e88178 (2014).
- Fu, Y. H. et al. Declining global warming effects on the phenology of spring leaf unfolding. *Nature* 526, 104–107 (2015).
- Maina, F. Z., Kumar, S. V. & Gangodagamage, C. Irrigation and warming drive the decreases in surface albedo over High Mountain Asia. Sci. Rep. 12, 16163 (2022).
- Picard, G. et al. Bud-burst modelling in Siberia and its impact on quantifying the carbon budget. Glob. Change Biol. 11, 2164–2176 (2005).
- Furey, G. N. & Tilman, D. Plant biodiversity and the regeneration of soil fertility. Proc. Natl Acad. Sci. USA 118, e2111321118 (2021).
- Mori, A. S. et al. Biodiversity-productivity relationships are key to nature-based climate solutions. Nat. Clim. Change 11, 543–550 (2021).
- Rheault, G., Lévesque, E. & Proulx, R. Diversity of plant assemblages dampens the variability of the growing season phenology in wetland landscapes. BMC Ecol. Evol. 21, 91 (2021).
- Yin, R. et al. Experimental warming causes mismatches in alpine plant-microbe-fauna phenology. Nat. Commun. 14, 2159 (2023).
- Wolf, A. A., Zavaleta, E. S. & Selmants, P. C. Flowering phenology shifts in response to biodiversity loss. *Proc. Natl Acad. Sci. USA* 114, 3463–3468 (2017).
- 17. Dronova, I., Taddeo, S. & Harris, K. Plant diversity reduces satellite-observed phenological variability in wetlands at a national scale. *Sci. Adv.* **8**, eabl8214 (2022).

- Chen, X. et al. Tree diversity increases decadal forest soil carbon and nitrogen accrual. *Nature* https://doi.org/10.1038/s41586-023-05941-9 (2023).
- Zhang, S., Dai, J. & Ge, Q. Responses of autumn phenology to climate change and the correlations of plant hormone regulation. Sci. Rep. 10, 9039 (2020).
- Liu, D., Wang, T., Peñuelas, J. & Piao, S. Drought resistance enhanced by tree species diversity in global forests. *Nat. Geosci.* 15, 800–804 (2022).
- Oliveira, B. F., Moore, F. C. & Dong, X. Biodiversity mediates ecosystem sensitivity to climate variability. *Commun. Biol.* 5, 628 (2022).
- García-Palacios, P., Gross, N., Gaitán, J. & Maestre, F. T. Climate mediates the biodiversity–ecosystem stability relationship globally. Proc. Natl Acad. Sci. USA 115, 8400–8405 (2018).
- Gould, I. J., Quinton, J. N., Weigelt, A., De Deyn, G. B. & Bardgett, R. D. Plant diversity and root traits benefit physical properties key to soil function in grasslands. *Ecol. Lett.* 19, 1140–1149 (2016).
- 24. Ding, J. et al. Decadal soil carbon accumulation across Tibetan permafrost regions. *Nat. Geosci.* **10**, 420–424 (2017).
- Chen, S. et al. Plant diversity enhances productivity and soil carbon storage. Proc. Natl Acad. Sci. USA 115, 4027–4032 (2018).
- Beugnon, R. et al. Tree diversity and soil chemical properties drive the linkages between soil microbial community and ecosystem functioning. ISME Commun. 1, 41 (2021).

- Zhang, J. et al. Variation and evolution of C:N ratio among different organs enable plants to adapt to N-limited environments. Glob. Change Biol. 26, 2534–2543 (2020).
- 28. Wang, C., Cao, R., Chen, J., Rao, Y. & Tang, Y. Temperature sensitivity of spring vegetation phenology correlates to within-spring warming speed over the Northern Hemisphere. *Ecol. Indic.* **50**, 62–68 (2015).
- Xin, Q. et al. A semiprognostic phenology model for simulating multidecadal dynamics of global vegetation leaf area index. J. Adv. Model. Earth Syst. 12, e2019MS001935 (2020).
- Shen, M. et al. Plant phenology changes and drivers on the Qinghai–Tibetan Plateau. Nat. Rev. Earth Environ. 3, 633–651 (2022).

Publisher's note Springer Nature remains neutral with regard to jurisdictional claims in published maps and institutional affiliations.

Springer Nature or its licensor (e.g. a society or other partner) holds exclusive rights to this article under a publishing agreement with the author(s) or other rightsholder(s); author self-archiving of the accepted manuscript version of this article is solely governed by the terms of such publishing agreement and applicable law.

@ The Author(s), under exclusive licence to Springer Nature Limited 2024

Methods

Biodiversity, climate and ancillary data

We focused our research on areas in the middle and high latitudes of the northern hemisphere (>30° N), where vegetation dynamics exhibit distinct seasonal variations. We extracted species richness data covering most of the forests in our study area from the GFBI ground observation dataset 31 to characterize biodiversity, which compiles extensive monitoring data from 777,126 permanent plots across 44 countries and 13 ecoregions. The GFBI dataset encompasses diverse forest sources and successional stages, and more than 30 million trees belonging to over 8,737 species were measured twice or more, with the aim of unveiling global forest biodiversity patterns.

Due to the large number of duplicate coordinates in the GFBI dataset, we used a window size of 0.01 degrees, the minimum scale of GFBI coordinate records, to extract the mean value within each window as its corresponding value. In the end, we determined 393,139 unique biodiversity records, encompassing 1–190 tree species. Among these plots, 75% were measured at two or more time points, with a minimum time interval between measurements of two years or more (the global average time interval is nine years), while 25% were measured only once. Due to the majority of plots being measured multiple times, the impact of sampling frequency on the results is probably minimal²⁰. Notably, deciduous broadleaf forests and woody savannahs exhibit the highest species richness per plot scale, averaging six to seven species per plot, while open shrublands, barren lands and grasslands contain only two to three tree species (Supplementary Fig. 1). We also used grid-form species richness data, which were simulated by the original authors of the GFBI dataset using machine learning techniques, ensuring spatial consistency with the structure of the climate dataset and other datasets.

The leaf-out dates were determined from the MODIS Land Cover Dynamics (MCD12Q2) dataset, which provides global land surface phenology metrics annually spanning from 2001 to 2022 with a spatial resolution of 500 metres³². These metrics are derived from time series data of the two-band Enhanced Vegetation Index (EVI2) computed from MODIS Nadir Bidirectional Reflectance Distribution Function-Adjusted Reflectance. One of these metrics, leaf-out dates, is defined as the date when the EVI2 first exceeds 15% of the segment EVI2 amplitude.

The climate data were obtained from monthly data of the ERA5-Land dataset, which is the fifth-generation atmospheric reanalysis produced by the European Centre for Medium-Range Weather Forecasts³³. It has been widely used for evaluating the influence of meteorological variables on the Earth's global climate. Specifically, we extracted temperature, total precipitation, solar radiation and soil moisture data from 2000 to 2022, with a spatial resolution of 0.1 degrees and a temporal resolution of one month from ERA5-Land. Furthermore, we collected hourly soil temperature data and calculated the daily mean for later analysis. We computed the multi-year average climate variables and spring average climate variables for each plot. Regarding spring average climate variables, we identified the optimal spring pre-season period through partial correlation analysis. We initiated the iteration from the month of the multi-year average leaf-out dates, moving forward continuously. In each iteration, we calculated the average variables of the current pre-season period and computed the correlation coefficient. We continued the iteration until the sixth month, selecting the optimal pre-season period with the maximum partial correlation coefficient.

The soil attribute data were derived from SoilGrids, a global soil dataset product resulting from international collaboration generated by the ISRIC—World Soil Information Center, with a resolution of 250 metres³⁴. SoilGrids implements advanced machine learning techniques, combining global soil profile data and environmental covariate data to predict and simulate the spatial distribution of soil properties at six standard depths globally. We used the latest version of SoilGrids, version 2.0, to extract soil surface organic carbon content and soil total nitrogen content, and subsequently calculated the soil surface C/N ratio.

The GPP data were originated from the Trendy and CMIP6 models, used for the simulation of leaf-out dates across historical and future periods. The Trendy model ensemble encompassed many models reflecting estimates of terrestrial vegetation photosynthesis and was extensively employed to delve into diverse facets of the global carbon cycle³⁵. We curated GPP data spanning from 2001 to 2021, encompassing 15 models (Supplementary Table 2). CMIP6 furnishes output data for an array of climate variables under different experimental designs and emission scenarios, encompassing historical and forthcoming epochs³⁶. We gathered GPP, temperature, precipitation, radiation and soil moisture data from 2015 to 2100 across each of 13 models. Each model encompasses three SSPs: SSP1-2.6, SSP2-4.5 and SSP5-8.5 (Supplementary Table 3).

Other auxiliary data included biomes, vegetation types, climate zones, forest age, elevation and species evenness. The biome data were derived from the Resolve Ecoregions 2017, which serves as a biogeographic regionalization under an Earth's biomes framework, consisting of 14 terrestrial biomes made up of 846 ecoregions, defining biogeographic assemblages and ecological habitats³⁷ (Supplementary Table 4). The vegetation type data were obtained from the first layer of the MCD12Q1 version 6.1 dataset and represent land cover types in the International Geosphere-Biosphere Programme classification³⁸ (Supplementary Table 5). The climate zone data were procured from the widely used Köppen-Geiger climate classification system, which divides the global climate zones into five primary groups on the basis of local vegetation types: tropical, arid, temperate, continental and polar³⁹. Further subdivisions of each group are based on temperature or aridity level (Supplementary Table 6). The forest age data were sourced from the Max Planck Institute for Biogeochemistry in Germany. These data provide global forest age estimations at a one-kilometre resolution and are predicted using machine learning techniques on the basis of forest inventories, biomass measurements and climate data. The elevation data were obtained from the Global Multi-resolution Terrain Elevation Data 2010, provided by the US Geological Survey Earth Resources Observation and Science Center. We selected the version with a 30-arc-second spatial resolution. We used Hill's evenness as an indicator of species evenness, which can be roughly interpreted as the proportion of species dominating the community in terms of abundance. These data were sourced from ref. 40, and evenness values range from close to zero (indicating domination by a few species) to one (indicating an equal number of individuals for all species in the community).

Simulating leaf-out dates using GPP data from the Trendy and CMIP6 models

We employed GPP data from the CMIP6 and Trendy models to simulate leaf-out dates. GPP exhibits a close correlation with factors such as vegetation coverage, leaf area index, temperature and precipitation—all pivotal elements influencing vegetative leaf-out dates. The annual fluctuation curve of GPP therefore effectively mirrors the phenological cycles of vegetation 41 . Drawing on this theoretical foundation, we used cubic spline interpolation for temporal sequence interpolation to enhance data continuity, considering that the temporal resolution of most GPP datasets is monthly. We then opted for the phenofit function package 42 in the R programming language for simulation. To ensure both efficiency and quality in simulating leaf-out dates, we employed the 'Elmore' curve fitting method 36 . The fitting function is represented by equation (1):

$$f(t) = mn + (mx - m_7 t) \times \left(\frac{1}{1 + e^{-rsp(t - sos)}} - \frac{1}{1 + e^{-rau(t - eos)}}\right)$$
 (1)

where *t* is the corresponding date of time series GPP; mn and mx are the minimum and maximum value of time series GPP; sos and eos denote the start of the growing season and the end of the growing season, respectively; rsp and rau are the rates of spring greenup and autumn

senescence, respectively; and m_7 is the summer greendown parameter. Subsequently, on the basis of the fitted curve, we used three different methods to extract leaf-out dates: the threshold method, the derivative method and the inflection method. Through meticulous comparisons, the extracted leaf-out dates exhibited harmonious interannual variations across all three methods (Supplementary Fig. 10). To maintain congruity with MCD12Q2, we chose to showcase the 15% threshold method as the primary approach in the main text.

Calculating S_T and RSWS

We first aggregated data from multiple sources using the coordinates from the biodiversity data. For climate data with coarser resolutions, we directly extracted data from the corresponding locations. For categorical datasets such as biomes, we used the mode within the corresponding window size as the representative value, while for continuous datasets such as soil properties, we used their mean values within the grid. We then standardized all data using the Z-score method to convert metrics of varying units into a uniform scale, and we excluded outliers in accordance with the PauTa criterion.

 S_T , the sensitivity of leaf-out advance to warming, is defined as the days of advanced leaf-out dates per degree of change in air temperature. For the purpose of narrative convenience, we defined the advancement of leaf-out dates as a positive value and the delay as a negative value, which is equivalent to taking the opposite of the temperature coefficient as S_T . It can be calculated using the coefficient of temperature in a regression that relates leaf-out dates to climate variables, as shown in equation (2):

$$L = \beta_0 + (-\beta_T) \times T + \beta_P \times P + \beta_R \times R + \varepsilon$$
 (2)

where L stands for leaf-out dates; T, P and R denote the mean spring temperature, precipitation and radiation, respectively; β_T , β_P and β_R represent their corresponding regression coefficients, of which β_T signifies S_T ; β_0 is the intercept; and ε is the residual term. To calculate mean spring values of climate variables, we employed a partial correlation method to iteratively determine the optimal length of the spring pre-season. To fit the regression equation, we used the OLS (ordinary least squares regression) function provided by the statsmodels 43 package in Python.

RSWS is defined as the speed of soil temperature change over a period of 60 days, including 30 days before and 30 days after the leaf-out date. To calculate RSWS, we first derived daily soil temperature data from hourly data between 2001 and 2021. We then used the Numpy⁴⁴ package in Python to fit the daily mean soil temperature data for the 60-day period in each plot, allowing us to determine the slope (that is, RSWS) as well as the variance, which represents the degree of temperature variability in each plot.

Analysis

We first used partial correlation and sequential regression methods to investigate the relationship between biodiversity and S_T across all plots (Fig. 1b). The partial correlation method was implemented using the pingouin⁴⁵ package in Python. When calculating partial correlation, we controlled for mean spring temperature, precipitation, radiation and soil moisture, as well as SOC, total nitrogen, forest age, elevation and evenness, to eliminate the influence of environmental factors. On the basis of the ordinary least squares regression method, we devised a sequential regression model to isolate the confounding effects of environmental covariates. We regressed biodiversity onto the environmental variables to obtain the residuals of biodiversity without the covariances of environmental variables. Subsequently, the residuals and environmental variables were regressed on S_T to estimate the coefficient of residuals (β_B , as described in equation (4)), which characterizes the relationship between biodiversity and S_T . This sequential regression model is expressed as:

$$\varepsilon_{\rm B} = B - (\beta_{\rm B} + \sum_{i=1}^{n} \beta_i \times X_i)$$
 (3)

$$S_{T} = \beta_{0} + \beta_{B} + \varepsilon_{B} + \sum_{i=1}^{n} \beta_{i} \times X_{i} + \varepsilon$$
(4)

where B is biodiversity, \mathcal{E}_B is the residual of biodiversity, X_i is environmental variable i, β_i is the regression coefficient of environmental variable i and ε is the residual term.

To mitigate the potential impact of spatial autocorrelation among variables, we employed two spatial autoregressive models to investigate the relationship between biodiversity and S_T . First, the spatial lag model introduced the lagged values of the dependent variable (that is, the values of the dependent variable in neighbouring locations) as explanatory variables to capture spatial dependence among adjacent locations. Second, the spatial error model assumed that the error terms of the model possess a spatial structure, indicating a certain level of spatial autocorrelation in the error terms across space. The analysis of these models was conducted using the spreg⁴⁶ package in Python.

Furthermore, we used the random forest and XGBoost machine learning algorithms, along with the SHAP method, to measure the impact and importance of biodiversity on S_T. Random forest and XGBoost are decision-tree-based machine learning algorithms that excel in processing large-scale data and high-dimensional features, effectively handling nonlinear relationships between features. We implemented these methods using the scikit-learn⁴⁷ and xgboost⁴⁸ packages in Python to explore the relationships between S_T , biodiversity and other environmental variables. While the random forest and XGBoost models offer the Gini coefficient as an importance metric, they fall short in illustrating the individual contribution of each feature in predicting results on a per-sample basis. To overcome this limitation, we used the SHAP method-a robust tool for interpreting machine learning models. Rooted in Shapley values from game theory, this method assesses the contribution of each feature value within various possible feature combinations. It ensures a fair distribution of the impact of each feature on the prediction results. Using the shap⁴⁹ package in Python, we applied the SHAP method to interpret the trained random forest and XGBoost models. This allowed us to obtain the magnitude and direction (positive or negative) of the impact of biodiversity on S_T of each plot (Fig. 1d and Supplementary Fig. 5). We then calculated the mean absolute SHAP values for each feature across all samples as a measure of feature importance, referred to as SHAP importance, as shown in Fig. 1c.

To address possible spatial heterogeneity issues at the global scale, we employed two approaches to conduct analyses at a smaller local scale. First, we divided our study area into different regions, including land cover types, biomes and climate zones. We then conducted partial correlation analysis on the data within each region. We also conducted point-wise analyses. To do this, we first created a distance matrix to group the points into clusters on the basis of their proximity to each other. Then, we used partial correlations to conduct the analysis. To select the points in each group, we used the golden section method as the search algorithm and the Akaike information criterion to determine the optimal bandwidth size. The significance was based on t statistics using a two-tailed test, and the Benjamini-Hochberg method was employed to control the false discovery rate. Due to the sparseness of point-form species evenness data, there are limitations in successfully matching it with point-form species richness data and significant S_T data, hindering further analysis. We therefore did not use it in the local analysis (Fig. 1a,e-j). To address this limitation, we introduced grid-form species richness data, which perfectly match with evenness data, supporting all analyses, and the conclusions remain consistent with the original findings (Fig. 1 and Supplementary Fig. 6).

To investigate the potential mechanisms underlying the impact of biodiversity on S_T , we used two methods at the point level; partial correlation and structural equation modelling. We hypothesized that the impact of biodiversity on S_T is mediated by its influence on soil physicochemical properties and tree root growth. To test this hypothesis. we developed an SEM incorporating six mediating variables: two soil physical properties (bulk density and VOCF), two soil nutrient variables (SOC and C/N ratio), RSWS and root depth. Maximum likelihood estimation was used as the target function, while the sequential least squares programming optimization method was employed to estimate the model parameters. We also calculated various statistics and fit indices to evaluate the applicability and effectiveness of the model, such as the goodness-of-fit index and the root mean square error of approximation. Subsequently, we selected pathways that surpassed the 0.9 threshold for the goodness-of-fit index and exhibited Benjamini-Hochberg-corrected *P* values below 0.05, calculating their respective mean values. We also used partial correlation analysis as a supplement to the SEM. While controlling for mean annual temperature, precipitation and solar radiation effects, we conducted partial correlation analyses on variables at both ends of each SEM path.

For the data from the Trendy and CMIP6 models, we followed the same procedure as described above to calculate S_T and analyse the impact of biodiversity on it. However, due to the coarse resolution and lack of time series in these models, temporal and regional analyses were not possible. To determine the biodiversity effects at each point, we employed the geographically weighted regression (GWR) method. GWR is a spatially local regression model that considers spatial heterogeneity. Throughout the analysis, due to the absence of future biodiversity, soil attribute and elevation data, we assumed they remained constant and resampled them to match the resolution of the models. We conducted year-by-year accumulation to obtain future forest age. Due to the sparseness of the point-form species evenness data, challenges arose in aligning them with coarse-resolution model data and point-form species richness data, hampering further analysis. We therefore did not use these data in the GWR analysis. We then conducted GWR to analyse the relationship between the models' S_{T} and factors including biodiversity, mean spring temperature, precipitation, radiation and soil moisture, as well as SOC, soil nitrogen, forest age and elevation. Simultaneously, we resampled the observed data to the same resolution as each model and calculated the impact of biodiversity on S_{τ} (Supplementary Fig. 11). Finally, we compared the biodiversity effect of the observed results and the Trendy and CMIP6 models, and assessed the accuracy of each model at the pixel scale (Fig. 3, Extended Data Fig. 1 and Supplementary Figs. 7-9).

Data availability

All the data used in this study are available online via the following links: GFBI, https://www.gfbinitiative.org/data; ERA5, https://doi.org/10.24381/cds.e2161bac; Trendy, https://blogs.exeter.ac.uk/trendy; CMIP6, https://esgf-node.llnl.gov/projects/cmip6; elevation, https://doi.org/10.3133/ofr20111073; SoilGrids, https://doi.org/10.5194/soil-7-217-2021; evenness, https://doi.org/10.3929/ethz-b-000597256; forest age, https://doi.org/10.5194/essd-13-4881-2021; MCD12Q1v061, https://doi.org/10.5067/MODIS/MCD12Q1.061; MCD12Q2v061, https://doi.org/10.5067/MODIS/MCD12Q2.061; Ecoregions 2017, https://ecoregions.appspot.com; Köppen–Geiger maps, https://doi.org/10.1038/s41597-023-02549-6. Source data are provided with this paper.

Code availability

All the code used for data analysis and figure generation is available on GitHub at https://github.com/spjace/asc-for-bio-effect-on-lud (ref. 50). Furthermore, we packaged this code into the Python package phenology for phenological analysis and computing optimal pre-season length, released on the Python Package Index at https://pypi.org/project/phenology.

References

- Liang, J. et al. Positive biodiversity-productivity relationship predominant in global forests. Science 354, aaf8957 (2016).
- Friedl, M. A., Gray, J. & Sulla-Menashe, D. MODIS/Terra+Aqua Land Cover Dynamics Yearly L3 Global 500 m SIN Grid V061 [MCD12Q2] (NASA EOSDIS Land Processes Distributed Active Archive Center, 2022).
- 33. Muñoz-Sabater, J. ERA5-Land Monthly Averaged Data from 1950 to Present (Copernicus Climate Change Service Climate Data Store, 2019).
- 34. Poggio, L. et al. SoilGrids 2.0: producing soil information for the globe with quantified spatial uncertainty. SOIL **7**, 217–240 (2021).
- 35. Yu, Z. et al. Forest expansion dominates China's land carbon sink since 1980. *Nat. Commun.* **13**, 5374 (2022).
- Zhu, B. et al. Constrained tropical land temperature–precipitation sensitivity reveals decreasing evapotranspiration and faster vegetation greening in CMIP6 projections. NPJ Clim. Atmos. Sci. 6, 91 (2023).
- 37. Dinerstein, E. et al. An ecoregion-based approach to protecting half the terrestrial realm. *BioScience* **67**, 534–545 (2017).
- Friedl, M. A. & Sulla-Menashe, D. MODIS/Terra+Aqua Land Cover Type Yearly L3 Global 500 m SIN Grid V061 [MCD12Q1] (NASA EOSDIS Land Processes Distributed Active Archive Center, 2022).
- Beck, H. E. et al. Present and future Köppen–Geiger climate classification maps at 1-km resolution. Sci. Data 5, 180214 (2018)
- Hordijk, I. et al. Evenness mediates the global relationship between forest productivity and richness. J. Ecol. 111, 1308–1326 (2023).
- Gonsamo, A., Chen, J. M. & D'Odorico, P. Deriving land surface phenology indicators from CO₂ eddy covariance measurements. *Ecol. Indic.* 29, 203–207 (2013).
- 42. Kong, D. et al. phenofit: an R package for extracting vegetation phenology from time series remote sensing. *Methods Ecol. Evol.* **13**, 1508–1527 (2022).
- 43. Seabold, S. & Perktold, J. Statsmodels: econometric and statistical modeling with Python. in *Proc. 9th Python in Science Conference* (eds van der Walt, S. & Millman, J.) 92–96 (2010).
- 44. Harris, C. R. et al. Array programming with NumPy. *Nature* **585**, 357–362 (2020).
- 45. Vallat, R. Pingouin: statistics in Python. J. Open Source Softw. 3, 1026 (2018).
- Rey, S. J. & Anselin, L. PySAL: A Python Library of Spatial Analytical Methods. in *Handbook of Applied Spatial Analysis* (eds Fischer, M. & Getis, A.) (Springer, 2010).
- 47. Pedregosa, F. et al. Scikit-learn: machine learning in Python. J. Mach. Learn. Res. 12, 2825–2830 (2011).
- Chen, T. & Guestrin, C. XGBoost: a scalable tree boosting system. in Proc. 22nd ACM SIGKDD International Conference on Knowledge Discovery and Data Mining 785–794 (Association for Computing Machinery, 2016).
- Lundberg, S. M. et al. From local explanations to global understanding with explainable AI for trees. *Nat. Mach. Intell.* 2, 56–67 (2020).
- 50. Shen, P. Python code for 'Biodiversity buffers the response of spring leaf unfolding to climate warming'. *GitHub* https://github.com/spjace/asc-for-bio-effect-on-lud (2024).

Acknowledgements

This work was funded by the National Natural Science Foundation of China (grant nos 42125101 and 42271034). X.W. was funded by the Youth Innovation Promotion Association of the Chinese Academy of Sciences (grant no. 2022051). Y. Zhang was funded by the National Natural Science Foundation of China (grant no. 42125105). J.P. was funded by the TED2021-132627B-IOO grant funded by the Spanish

MCIN, AEI/10.13039/501100011033, and by the European Union NextGenerationEU/PRTR, the Fundación Ramón Areces project no. CIVP20A6621 and the Catalan government grant no. SGR221-1333. C.M.Z. was funded by SNF Ambizione grant no. PZ00P3_193646. J.L. was supported by Science-i, of which the cyberinfrastructure was partially sponsored by the National Science Foundation of the United States (award no. 2311762).

Author contributions

C.W. designed the research. C.W. and P.S. wrote the first draft of the paper. P.S. and X.W. performed the data analysis. All authors assessed the research analyses and contributed to the writing of the paper.

Competing interests

The authors declare no competing interests.

Additional information

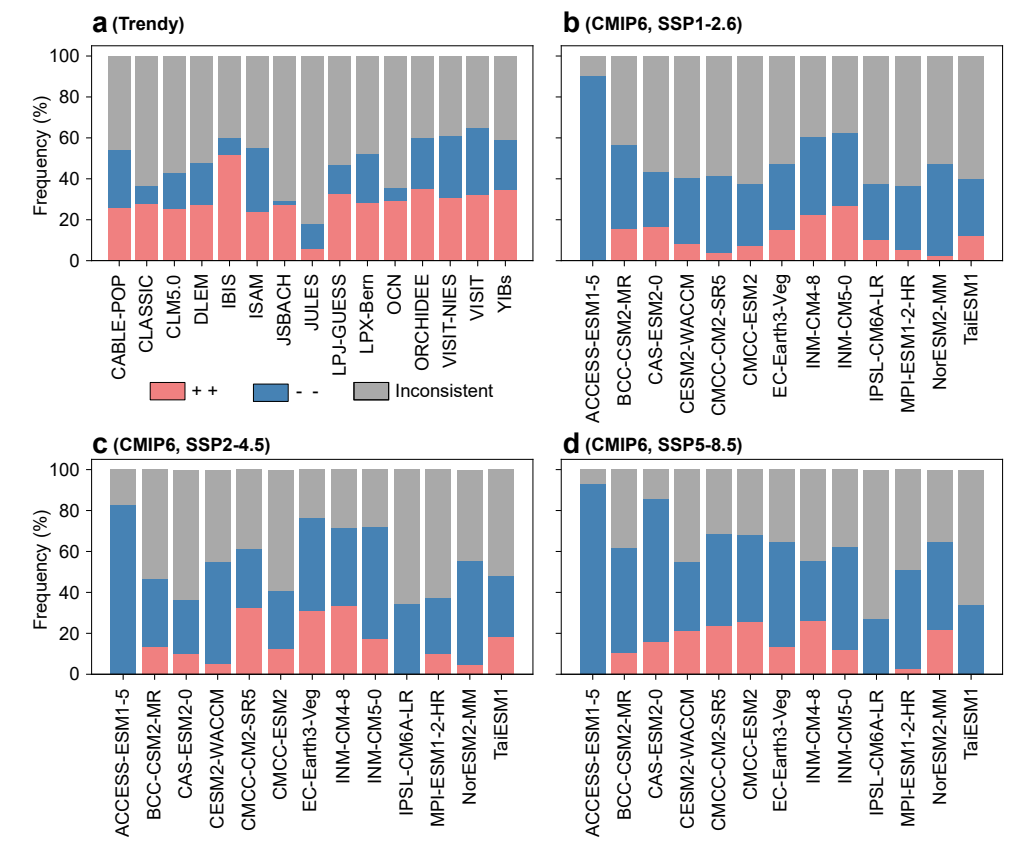
Extended data is available for this paper at https://doi.org/10.1038/s41558-024-02035-w.

Supplementary information The online version contains supplementary material available at https://doi.org/10.1038/s41558-024-02035-w.

Correspondence and requests for materials should be addressed to Weiwei Sun, Yongguang Zhang or Chaoyang Wu.

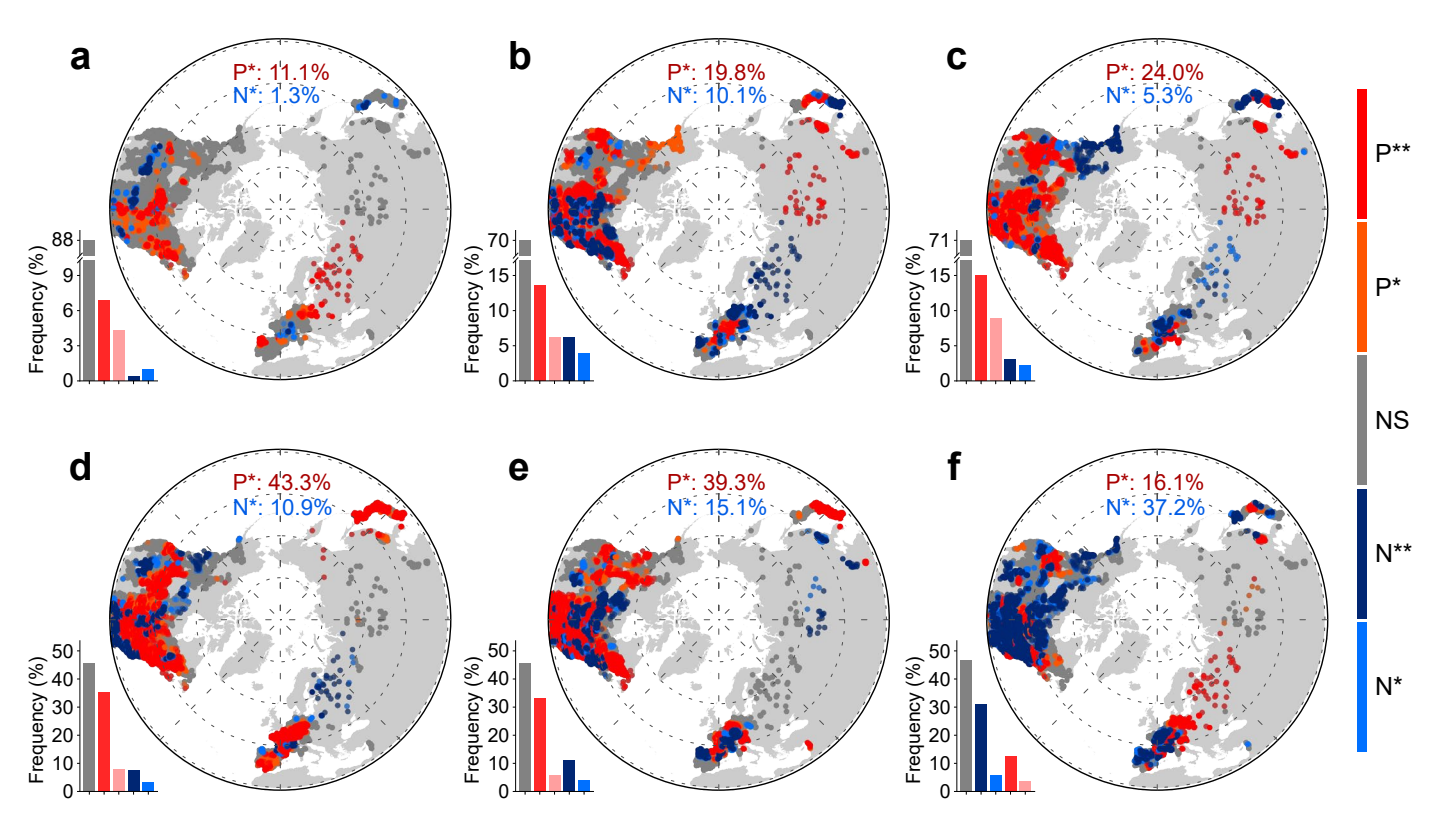
Peer review information *Nature Climate Change* thanks Yanjun Du and the other, anonymous, reviewer(s) for their contribution to the peer review of this work.

Reprints and permissions information is available at www.nature.com/reprints.



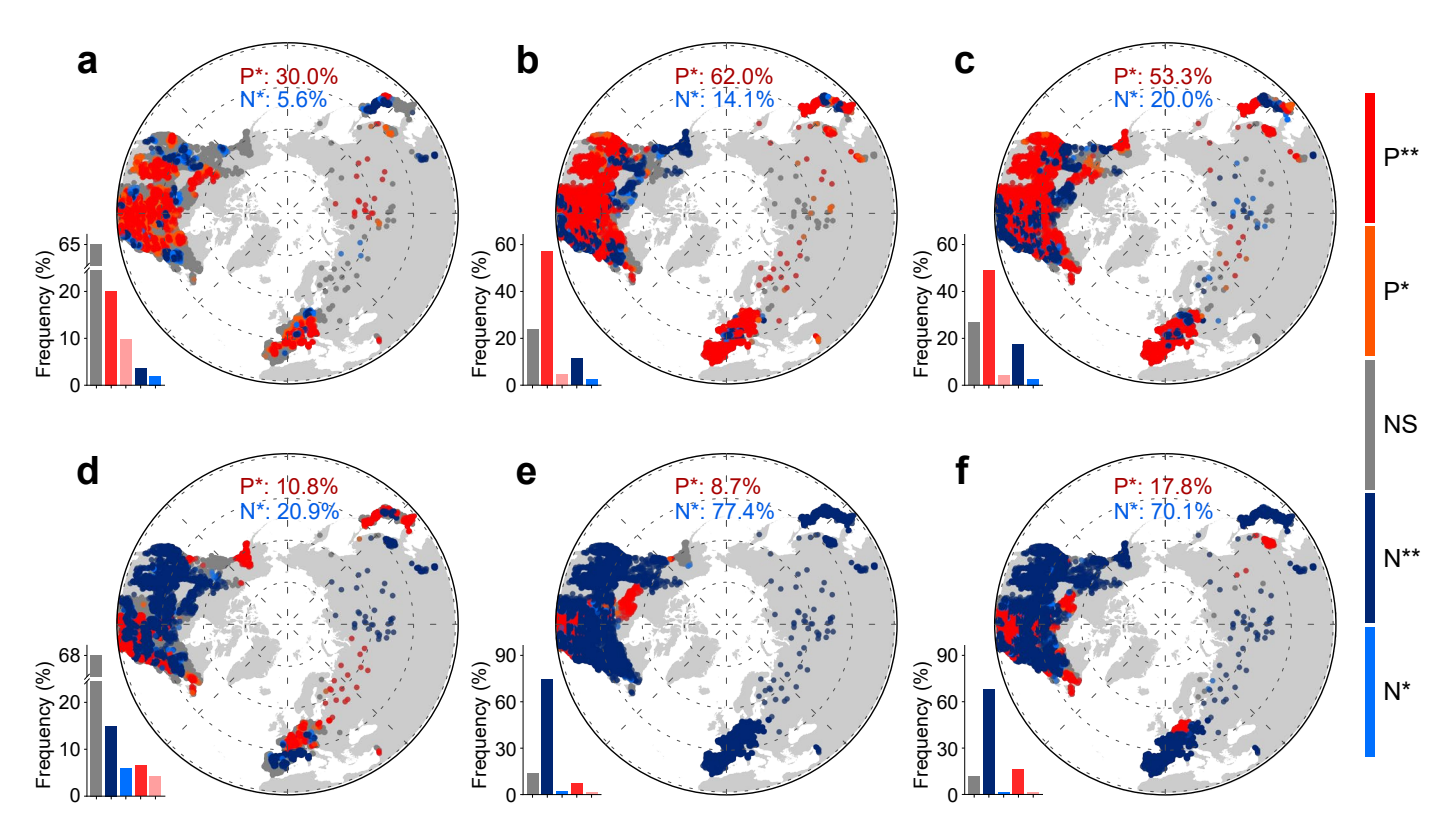
Extended Data Fig. 1| Spatially consistent evaluation of model performances on the sensitivity of spring leaf unfolding to warming (S_T) with biodiversity. a-d represent results for 15 Trendy models and 13 CMIP6 models under different

shared socioeconomic pathways (SSP1-2.6, SSP2-4.5 and SSP5-8.5), respectively. ++, The model outcomes correspond harmoniously with the observed results, exhibiting a positive correlation; --, both are negative.



Extended Data Fig. 2 | Biodiversity impacts soil moisture and organic carbon (SOC) by influencing root depth, consequently shaping the sensitivity of spring leaf unfolding to warming (S_T) . a-f, represent Partial correlation analysis results between biodiversity and root depth (a), biodiversity and spring soil moisture (b), biodiversity and SOC (c), root depth and soil organic carbon

 $\label{eq:continuous} \textbf{(d)}, root depth and spring soil moisture (\textbf{e}), spring soil moisture and S_T (\textbf{f}), respectively. The significance was based on the t statistics using a two-tailed test and to control the false discovery rate, the Benjamini-Hochberg (BH) method was employed in$ **a-f.***, \$P<0.05; **, \$P<0.01; NS, not significant; \$P\$, positive effect; and \$N\$, negative effect.



Extended Data Fig. 3 | Enhancing soil fertility through the Influence of biodiversity on soil physicochemical properties. a-f, represent the partial correlation analysis results between biodiversity and volumetric fraction of coarse fragments (VOCF) (a), VOCF and soil organic carbon (SOC) (b), VOCF and soil total nitrogen (N) (c), biodiversity and Soil pH (d), Soil pH and SOC (e), Soil

pH and N (\mathbf{f}), respectively. The significance was based on the t statistics using a two-tailed test and to control the false discovery rate, the Benjamini-Hochberg (BH) method was employed in \mathbf{a} - \mathbf{f} .*, P<0.05; **, P<0.01; NS, not significant; P, positive effect; and N, negative effect.